A FEM Assessment on the use of t-z and q-z Functions for Deep Foundations

Q.J. Ong[1], S.A. Tan[2]
[1,2]*Department of Civil & Environmental Engineering, National University of Singapore, Singapore*
E-mail: joshuaong@u.nus.edu

ABSTRACT: Load-movement t-z and q-z functions have been established and widely accepted as a tool to characterise pile shaft and toe resistances respectively. The functions are best used to represent a short element along the pile. But the question remains whether these functions depend on pile diameter and pile depth. This paper discusses the soil-structure interaction and load transfer mechanisms of a single pile and reviews the theoretical basis of the t-z and q-z functions. The bearing behaviour of a single circular footing under various conditions was also investigated and compared against the toe behaviour of piles. Linear elastic and Mohr-Coulomb soils are used for this study to investigate stress versus normalized movement curves for pile behaviour.

Keywords: Shallow foundation, Deep foundation, Piling, t-z, q-z

1. INTRODUCTION

Resistance versus movement curves or load-movement curves for shaft and toe resistances are referred as "t-z" functions for shaft resistance and "q-z" functions for toe resistance. Pile loading test results can be interpreted to characterise the pile behaviour by using t-z and q-z functions that represent the response in specific soil layers of a short pile element (Fellenius, 2019).

In finite element programs, "t-z" and "q-z" functions are an outcome of the calculations rather than a user input. The functions defined are consistent with the laws of mechanics; they satisfy equilibrium, compatibility, material constitutive behaviour and the defined boundary conditions. Finite element models are able to distinctly separate the head, shaft and toe load-movement behaviours of piles, which make the results ideal for detailed evaluation of "t-z' and "q-z" functions.

This paper aims to relook into the load transfer mechanisms of a footing and a single pile in homogenous soil conditions. The first part of the paper discusses the bearing behaviour of shallow foundations with respect to various footing sizes, subsequently, to be compared with the toe bearing of piles. Following which, head down tests on a single pile in homogenous soil with various strength profiles and various pile diameters are simulated to investigate the performance of the piles and their respective "t-z" and "q-z" functions. Finite element package PLAXIS 2D 2018 was used to analyse the shallow footings and piles. The study considers footings and pile foundations under various conditions as summarised in Table 1. The assumptions adopted in this paper are meant for a theoretical study to isolate mechanisms for detailed investigation.

Table 1 Summary of analyses

Case	Conditions	Weight of soil	Strength parameters	Figures
Footing #1	Linear elastic	20 kN/m^3	-	1, 2, 3, 4
Footing #2	Constant strength	20 kN/m^3	$s_u = 50kPa$	5, 6, 7, 8
Footing #3	Strength increasing with depth	20 kN/m^3	$c' = 1kPa, \phi = 32°, \psi = 0$	9, 10, 11, 12
Footing #4	N_γ omitted (non-associated flow rule)	0 kN/m^3	$c' = 100kPa, \phi = 32°, \psi = 0$	13
Footing #5	N_γ omitted (associated flow rule)	0 kN/m^3	$c' = 100kPa, \phi = \psi = 32°$	14, 16
Footing #6	N_γ & N_c omitted (associated flow rule)	0 kN/m^3	$c' = \sim 0kPa, \phi = \psi = 32°$	15
Pile #1	Constant strength	20 kN/m^3	$s_u = 50kPa$	17 to 29
Pile #2	Strength increasing with depth	20 kN/m^3	$c' = 1kPa, \phi = 32°, \psi = 0$	30 to 35

2. SHALLOW FOUNDATIONS

A finite element axisymmetric model was created to study the effect of footing size on load-movement curves, and to investigate the possibility of normalizing the behaviours of footings of various sizes. The FEM mesh has 4810 elements and 39050 nodes, and the geometrical size of the mesh is 40 m by 40 m. In this hypothetical scenario, linear elastic circular footings of dimensions 800 mm, 1500 mm and 2000 mm were studied. The footing material has a unit weight of 24 kN/m3, and the Young's modulus is 32 GPa.

The deformation properties of the soil are fixed with Young's modulus of 25 MPa, and a Poisson's ratio of 0.3. Unit weight of the soil is 20 kN/m3. The study is separated into three distinct strength profiles, where the first scenario follows a footing on linear elastic soil, the second scenario follows a footing on soil with constant strength, and the third scenario follows a footing on soil with varying strength with depth.

Prescribed line displacements were used to simulate loading on the footing. The displacements were modelled in 1 mm prescribed displacement loading stages up to 10 mm. Displacement control was chosen as opposed to stress control input so that the stiffness of the footing has a less influence on the problem. Displacement control is a model of a perfectly rigid footing. Under stress control loading schemes, footings of the same thickness but different diameter can have different inherent stiffness. The bending of the flexible footing can then be another variable in this study, which can change soil response significantly.

Figure 1 shows the contours of volumetric strain that each footing exerts on a linear elastic soil. The bearing behaviour can be normalized as the shear strain contours display similitude.

Figure 2 describes the load-movement curve of each footing diameter. As expected, the load carried by the footing increases as the diameter increases. Figure 3 shows the stress-movement curve of the same footings. The reverse is observed, where the smallest diameter carries the largest stress. Furthermore, the larger footing needs to move more than the smaller footings to obtain similar stress levels.

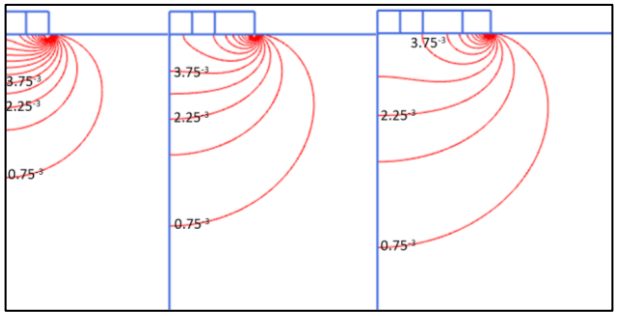

Figure 1 Contours of volumetric strain for footing sizes 400 mm, 800 mm and 1500 mm diameter on linear elastic soil (Maximum compressive volumetric strain: 1.5^{-2}, 20 intervals)

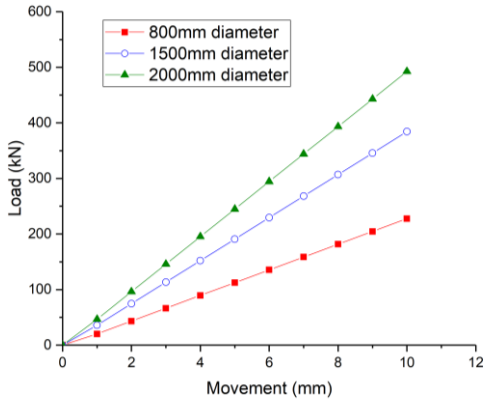

Figure 2 Load-movement curves for the various footing sizes on linear elastic soil

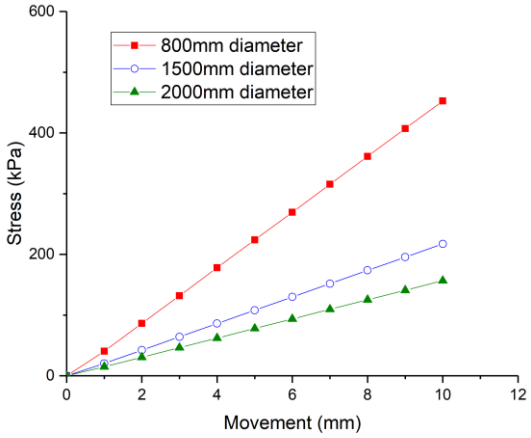

Figure 3 Stress-movement curves for the various footing sizes on linear elastic soil

Normalization is achieved by dividing the footing movement by the diameter to obtain a pseudo stress-strain curve, where the gradient of the curve is proportional to stiffness. The normalized curves, shown in Figure 4, show good agreement between the footings of different diameters.

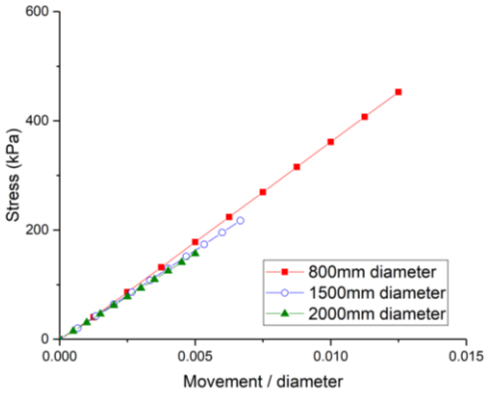

Figure 4 Stress vs. normalized movement for footings on linear elastic soil

For the following set of footings, a single homogenous soil layer is modelled by the well-known linear elastic perfectly plastic Mohr-Coulomb model. The model is based on Hooke's law of isotropic elasticity and employs a non-associated plasticity framework.

Figures 5, 6 7 and 8 show the various responses on soil with Undrained(B) type of strength. Total stress analysis is performed for a case of constant undrained shear strength of 50 kPa.

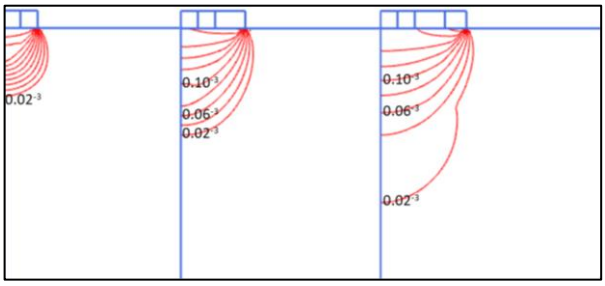

Figure 5 Contours of volumetric strain for footing sizes 400 mm, 800 mm and 1500 mm diameter on soil with constant strength (Maximum compressive volumetric strain: 4^{-4}, 20 intervals)

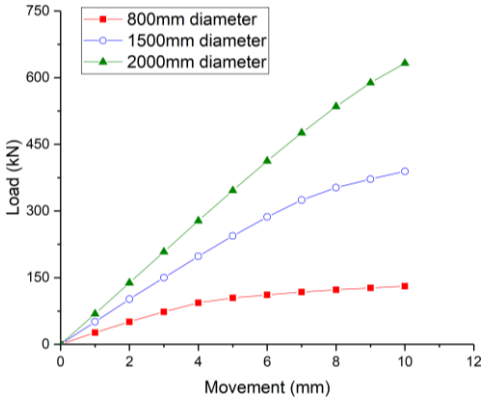

Figure 6 Load-movement curves for the various footing sizes on soil with constant strength

Similar trends from the constant strength analysis are observed as compared to the linear elastic footing, except for the influence from the onset of plasticity. This observation is further discussed in the third and final set of analyses for footings where a frictional material represents the soil. The strength properties of the soil then are effective cohesion of 1 kPa, and effective angle of friction of 32 degrees. Figures 9, 10 and 11 show the load movement curves when a frictional soil is used.

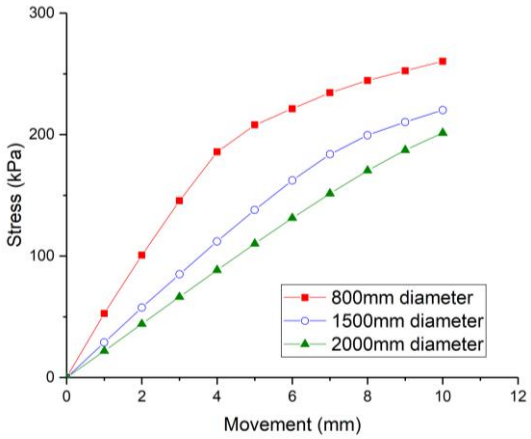

Figure 7 Stress-movement curves for the various footing sizes on soil with constant strength

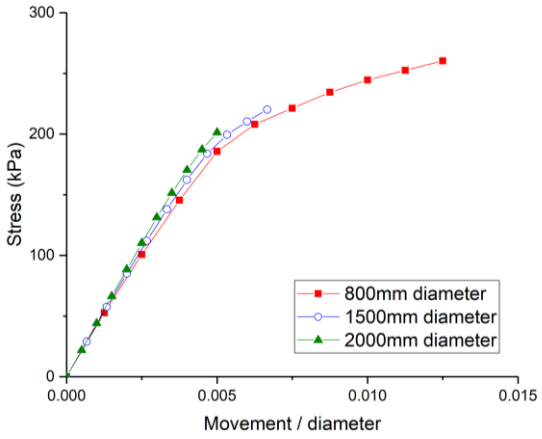

Figure 8 Stress vs. normalized movement for footings on soil with constant strength

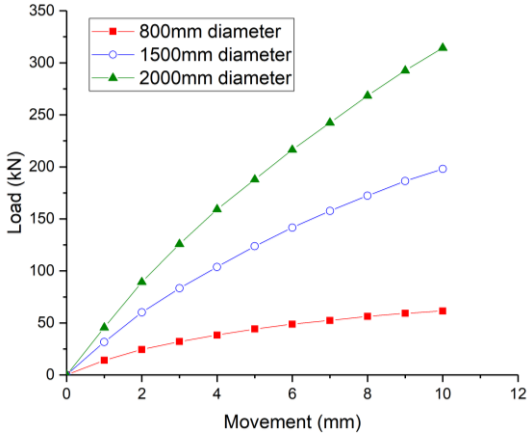

Figure 9 Load-movement curves for the various footing sizes on soil with varying strength with depth

With the Mohr-Coulomb model, the varying strength is given by $\tau = c + \sigma' tan\phi$. Where c is the cohesion, σ' is the effective normal stress and ϕ is the angle of friction. In a frictional soil, the strength of the material close to the ground surface will be small, as there is little confining stress. To maintain computational stability, a cohesion value of 1 kPa is given to the soil.

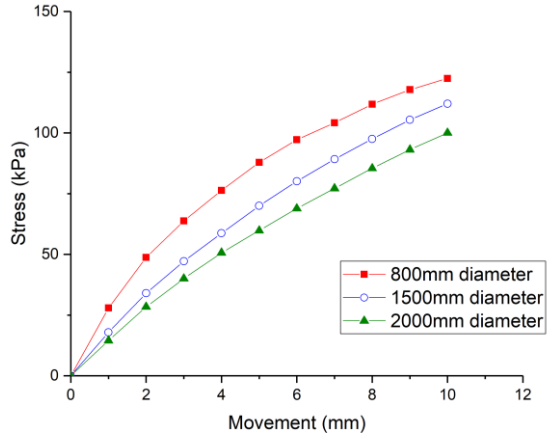

Figure 10 Stress-movement curves for the various footing sizes on soil with varying strength with depth

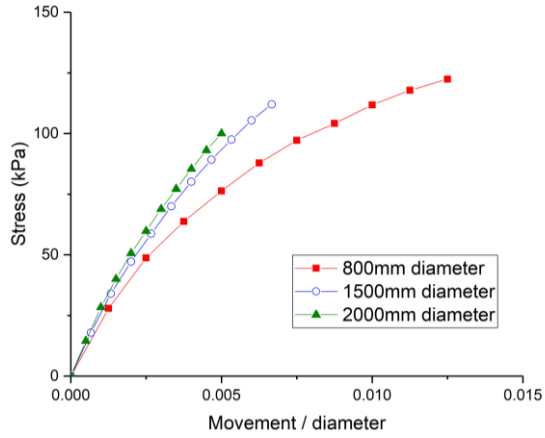

Figure 11 Stress vs. normalized movement for footings on soil with varying strength with depth

Figure 12 compares the various volumetric strain profiles beneath the footings. The depth of influence of the smaller footing is much smaller than the larger footing. It was also observed that under normal circumstances when footing is large enough, the divergence between the normalized curves decreases.

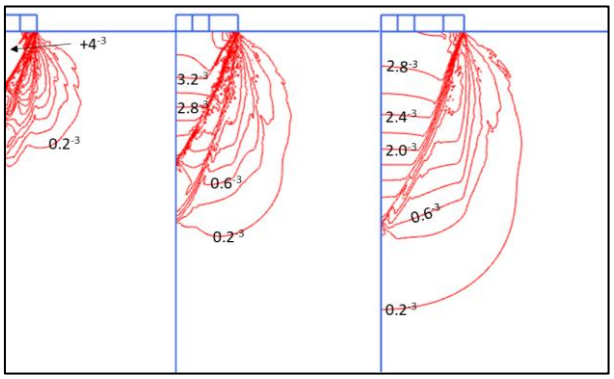

Figure 12 Contours of volumetric strain for footing sizes 400 mm, 800 mm and 1500 mm diameter on soil with varying strength with depth (Maximum compressive volumetric strain: 4^{-3}, 20 intervals)

After viewing these results, one might question, why then the numerical results of the footing on frictional soil cannot be normalized for these stress-strain plots? One of the possible reasons for being unable to normalize is the non-associativity of the constitutive model used. To some extent, the question of associated or non-associated plasticity is theoretically important for a frictional material. A non-associated plasticity condition is obtained when the dilation angle is not coincident to the angle of friction, whereas an associated plasticity condition happens when the dilation angle equals to the angle of friction. In non-associated plasticity, the bearing capacity (defined as the condition of plastic response having developed in the main portion of the affected soil body) is not independent of the footing size. The following series of figures show that even the simplistic Mohr-Coulomb model can give issues.

Early works by predecessors in soil mechanics found in theory that load-settlement curves can be normalized to be independent of footing size, by plotting a stress versus movement over diameter curve. Osterberg (1947) and Skempton (1951) studied effects of footing width on clay, Palmer (1948) on pavement, and more recently Briaud (1999) on sand. Perhaps a reason why normalization can be achieved in theoretical models was because rigid plastic and fully associative models were used in all their analyses. Even with a frictional soil, convergence can still be obtained if associated plasticity is assumed. Normalization is difficult to obtain once the problem is non-associative.

This explains why for footing design, just one N_c factor can cater to all cases regardless of footing size. When a frictional soil is encountered, the associative flow-rule complicates things. Real sand and gravel have dilative effects, which suggests that the issue at hand is no longer associative. Clayey cohesive soil for which the strength being characterized with Undrained(B) is less problematic.

The capability of numerical modelling enables the investigation of effects of associative and non-associative plasticity. The moment non-associativity is dealt with, which is the real behaviour of most frictional soil, then normalized bearing plots becomes questionable.

The general bearing capacity equation defined by Terzaghi (1943), Equation 1, superimposes the contribution of three basic components. The three components are soil strength, uniform surface surcharge, and soil self-weight.

$$q_u = cN_c + qN_q + \frac{1}{2}\gamma BN_\gamma \qquad (1)$$

Briaud and Gibbens (1997) pointed out that if the stress vs movement/diameter curve is unique for a given deposit, then the bearing capacity, q_u is independent of the footing width. For footings at the surface of a frictional material like sand, the general bearing capacity equation gives: $q_u = \frac{1}{2}\gamma BN_\gamma$. Here if $\frac{1}{2}\gamma BN_\gamma$ is a constant that is independent of B, then N_γ cannot be a constant and must carry a scale effect in l/B.

The contributions from the other bearing capacity components are then investigated, while isolating the contribution from the soil's self-weight. The approach of investigation follows that discussed by Griffiths (1982). The N_q component is considered by applying a 20 kPa surcharge on the top soil surface of the model. The N_c component is considered by assuming a large cohesion value of 100 kPa. Associativity is modelled by assuming the dilatancy angle is the same value as the friction angle, a value of 32 degrees.

For the same set of parameters other than associated plasticity, it was observed that the calculation with associated flow rule manages to collapse the curves to a narrower band, Figures 13 and 14.

When the cohesion is set to 0 kPa; with only the contribution due to N_q (uniform surface surcharge), the curves start to diverge after a certain strain level, as shown in Figure 15. This indicates that the contribution due to the N_c factor is critical for the normalization of the curves.

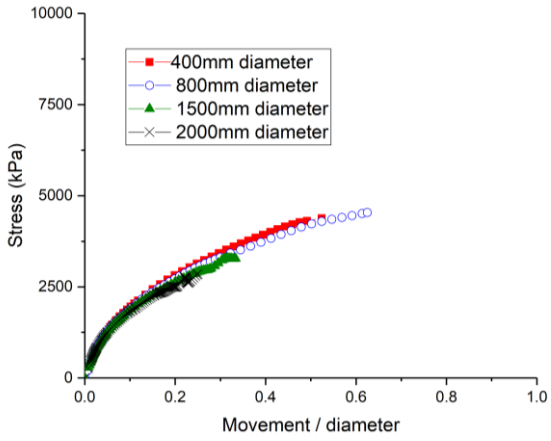

Figure 13 N_γ component omitted (non-associated flowrule)

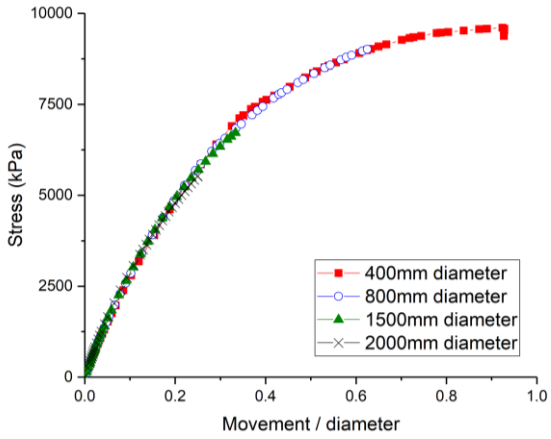

Figure 14 N_γ component omitted (associated flowrule)

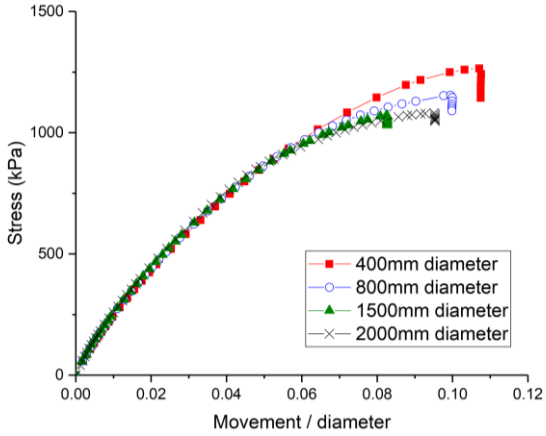

Figure 15 N_γ & N_c component omitted (associated flowrule); only contribution from uniform surcharge is considered

From these figures it can be said that for almost perfect normalization of the stress vs movement/diameter curves, two basic ingredients are necessary: associated flow rule and the omission or a small contribution of the N_γ component. Cohesive soils are more likely to exhibit a well-defined collapsed stress versus movement/diameter ratio as opposed to granular soils, where divergence eventually occurs at a larger strain.

The volumetric strain contours for the footing on soil with N_γ component omitted and associated flowrule is assumed, presented in Figure 16, show much better similitude in comparison to those when a non-associative flow was assumed, Figure 12, which is one of the reasons why normalizing the curves is possible.

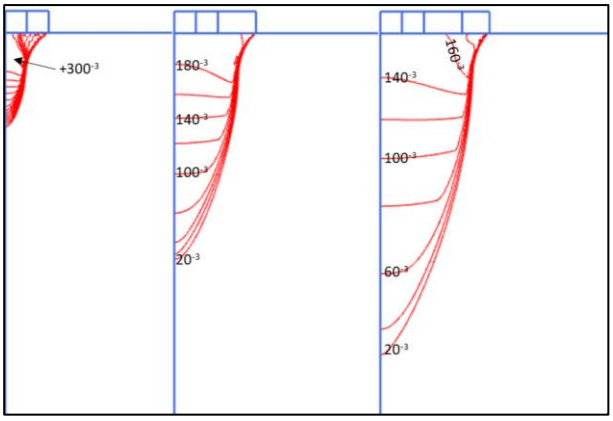

Figure 16 Contours of volumetric strain for the footing model when N_γ component omitted and associated flowrule is assumed (Maximum compressive volumetric strain: 4^{-1}, 20 intervals)

3. SINGLE PILE BEHAVIOUR IN HOMOGENOUS SOIL WITH CONSTANT STIFFNESS AND CONSTANT STRENGTH

This section address piles with diameters of 400 mm, 800 mm and 1500 mm that are loaded by 1 mm prescribed head displacement loading stages until 25 mm head movement is achieved. Total stress analysis with Undrained(B) type of strength is performed with undrained shear strength of 50 kPa. The pile is a linear elastic pile and has a density of 24 kN/m^3, and a Young's modulus of 32 GPa. The soil deformation properties were similar to those used in the footing study, that is, elastic-plastic shaft shear resistance. Figure 17 shows the finite element setup. The FEM mesh has 3532 elements and 29038 nodes, and the geometrical size of the mesh is 40 m by 40 m. The importance of the interface element is discussed later for the shaft resistance.

Figures 18, 19 and 20 show the load distribution curves for the three different pile sizes. The toe resistance and shaft resistance will be discussed separately, starting with the toe resistance.

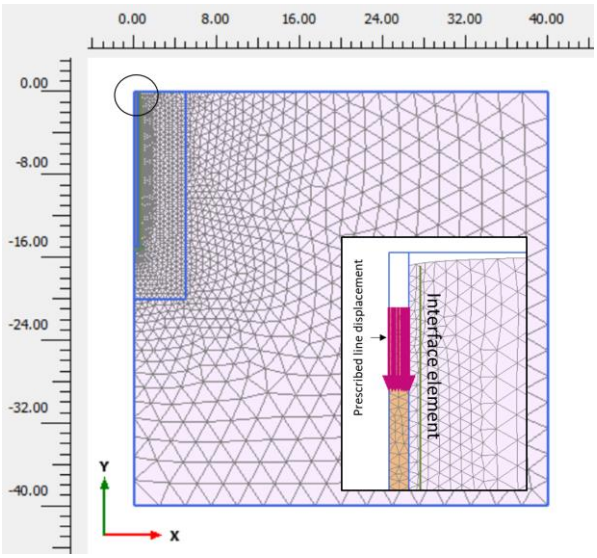

Figure 17 Finite element model mesh (dimensions in meters)

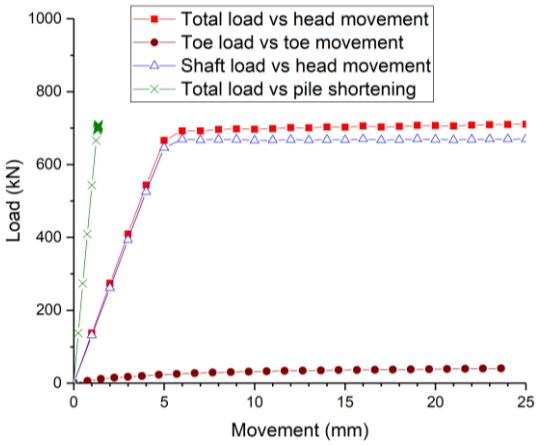

Figure 18 Load-movement for 400 mm diameter pile

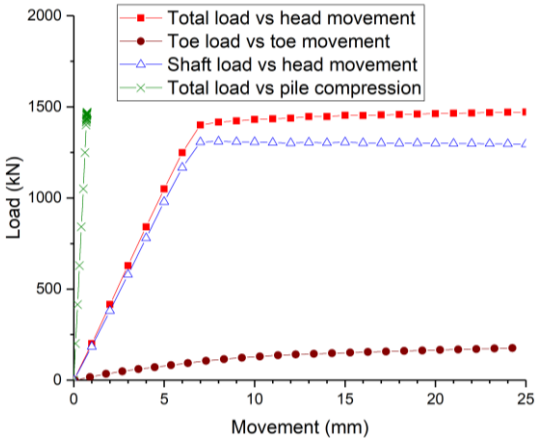

Figure 19 Load-movement for 800 mm diameter pile

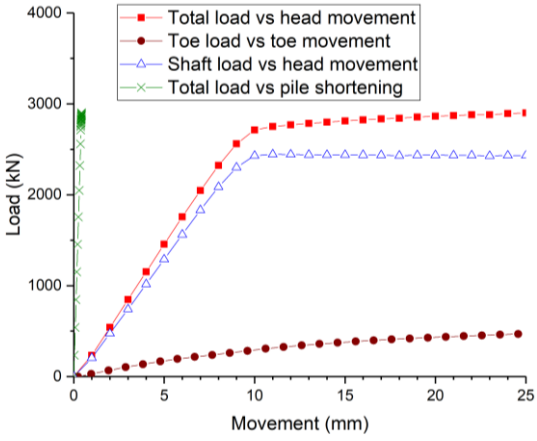

Figure 20 Load-movement for 1500 mm diameter pile

3.1 Toe resistance

The toe load-movement curves from each pile are plotted together in Figure 21. The overall toe behaviour is similar to observed behaviour in shallow raft foundations and plate load tests, where the bigger diameter experiences a softer response, but it can be loaded further to a higher value.

It is expected that a larger footing carries a bigger force for the same displacement. But using the concepts of Terzaghi's subgrade modulus, the reverse effect is obtained. Stress vs movement relations are similar to subgrade modulus, which does not have consistent units for normalized plots; when comparing Figures 22 and 23. In the

design of most shallow foundations using structural software (like SAFE), Winkler spring models are used. However, the approach goes against the fundamental understanding of foundations, where the bigger the foundation the more movement is needed to mobilize the same stress.

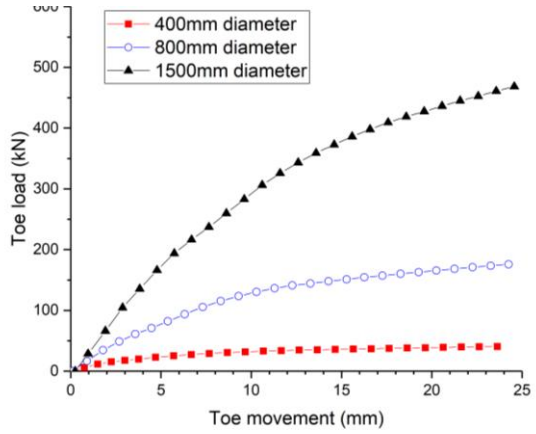

Figure 21 Toe load vs. toe movement for various pile diameters

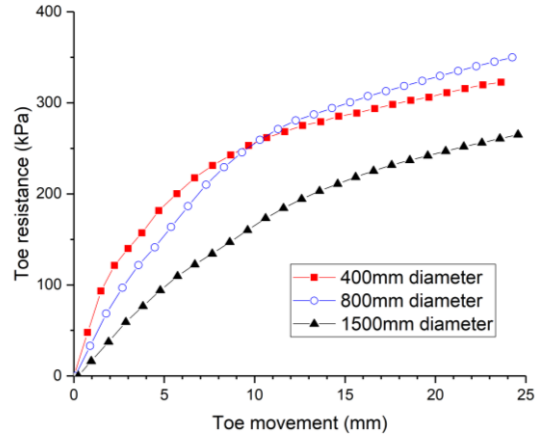

Figure 22 Unit toe stress vs. toe movement for various pile diameters

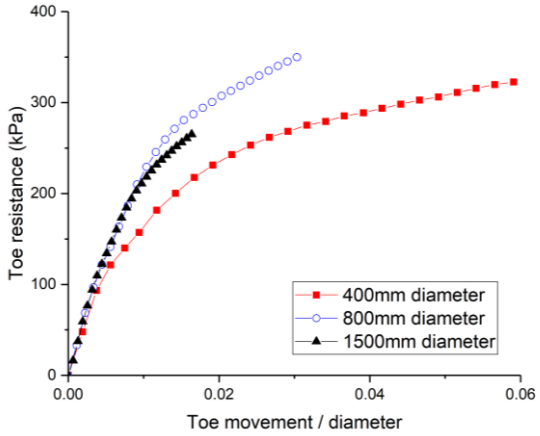

Figure 23 Unit toe resistance vs. normalized toe movement for various pile diameters

When normalizing both axes by transforming into a pseudo stress-strain plot, the curve should be coincident. In essence, the toe resistance of piles happens to be similar to that of shallow footings, except that the embedment effect becomes more prominent. The conditions for normalization of shallow footings have been discussed in the earlier sections.

Another hypothesis for the reason of variation in toe behaviour in piles for the different pile diameters is apart from the mechanics of associated plasticity. On loading a pile, the yielding zone is not similar to the shallow bearing capacity problem as mentioned due to the embedment effect. For each variation of pile size, the failure obtained does not display exact similitude. As the diameter of the pile varies, the smaller diameter has a small loaded volume. Where the volume of the plasticized zone would be proportional to the diameter of the footing, it will not follow proportionality for the toe of a pile. Figure 24 shows the contours of volumetric strain for the various pile diameters. Due to the embedment effect, the plots have slightly different contours and similitude is not obtained. This might explain why in the stress plot in Figure 22, the 400 mm diameter pile exhibits an unexpected response and crosses over the 800 mm diameter pile.

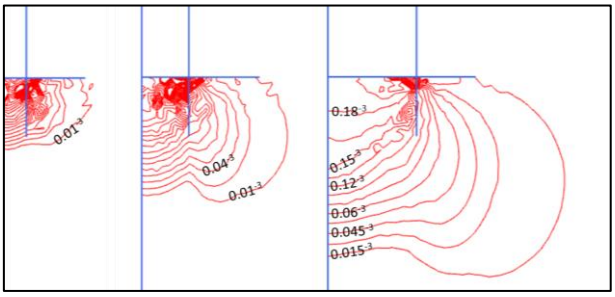

Figure 24 Contours of volumetric strain at the pile toe for diameters 400 mm, 800 mm and 1500 mm
(Maximum compressive volumetric strain: 3^{-3}, 20 intervals)

3.2 Shaft resistance

Following toe resistance, the shaft resistance of the pile is compared for the various diameters. In order to model the shaft behaviour of piles correctly, an interface element has to be included to capture the soil-structure interaction. In each interface element, Newton-Cotes integration were used instead of Gauss integration in Plaxis (Brinkgreve et al., 2018). As 15 noded elements were used in this set of analyses, each interface element would then have five pairs of nodes, where the positions of the stress points coincide with those of the node pairs. Each node pair would have identical coordinates in the finite element formulation, implying that the interface element has zero thickness. The interface elements allow for slipping, and slip will occur as the pile is much stiffer than the soil. The slippage is calculated by multiplying the shear stress at the interface by the virtual thickness of the interface, divided by the shear modulus of the interface element.

An R_{inter} parameter is used to determine the shear modulus of the interface element G_i, shown in equation 2. An R_{inter} value of 1 implies a rigid interface, where the interface properties would be the same as the soil properties adjacent to it. A R_{inter} value of 0.7 is adopted throughout this study to represent a normally rough interface.

$$G_i = R^2{}_{inter} G_{soil} \tag{2}$$

The R_{inter} value is also used to characterize the interface strength where values are scaled from the surrounding soil, as shown in equations 3 and 4. Likewise in the undrained scenario, cohesion is replaced by undrained shear strength.

$$c_i = R_{inter} c_{soil} \tag{3}$$

$$tan\ \varphi_i = R_{inter} tan\varphi_{soil} \tag{4}$$

After applying the prescribed displacement at the pile head, the relative displacement between pile and soil can be obtained subtracting the displacement of the node pairs in each interface.

The plot of shaft resistance against relative displacement is shown in Figure 25. Right at the interface, the rate of mobilisation of shaft resistance is independent of diameter. For this particular soil model and strength profile, slippage occurs at around 1.26 mm from the unit shaft resistance against relative movement, same for all the pile diameters and at all depths. This shows that for this particular pile in this particular soil, a single t-z function can represent the entire shaft resistance behaviour.

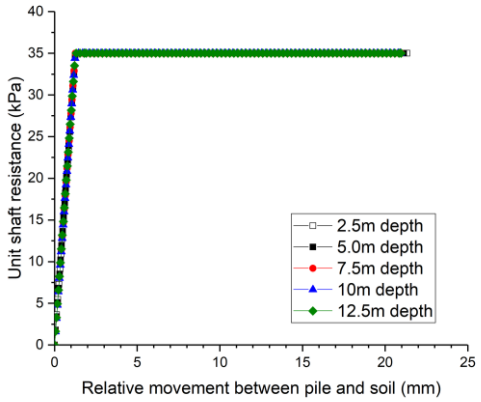

Figure 25 Unit shaft resistance against relative movement

The overall shaft resistance is obtained by deducting the toe loading from the total load. The shaft loads are then plotted with head movement of the pile, Figure 26. When plotted against pile head displacement, observations are similar to Mark Randolph's theory (Fleming et al., 2014), expressed in Equation 5.

$$\omega = \int_r^{r_m} \frac{\tau_0 r_0}{Gr} dr = \frac{\tau_0 r_0}{G} \ln\left(\frac{r_m}{r}\right) = \frac{\tau_0 d}{2G} \ln\left(\frac{r_m}{r}\right) \quad (5)$$

Where ω is the deflection of the pile, r_m is the maximum radius where the deflections in the soil become negligible, τ_0 is the limiting shear stress on the pile shaft, and r_0 is the pile radius.

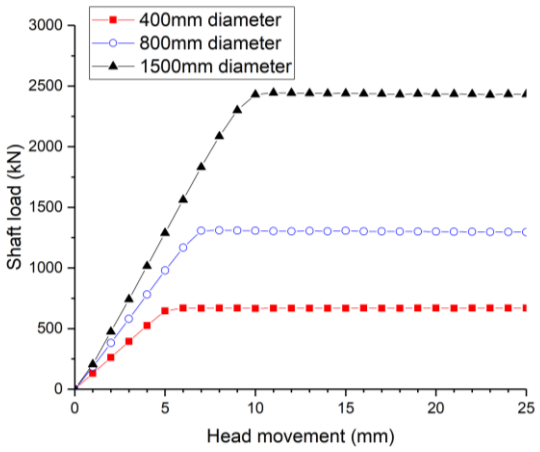

Figure 26 Load-movement curve for the shaft resistance

It should be noted that the deflection of pile is the absolute movement of pile shaft, not the relative movement of pile against soil. The theory assumes an elastic model with no interface element; the pile and soil are fully connected to each together. When using elastic theory, the soil moves together with the pile during compression. The soil is looped around the pile as a coaxial cylinder, and the elastic theory is used to calculate the movement of the coaxial cylinder. In this theoretical model, the pile movement with a fixed shear stress must then be a function of radius. In other words, for vertical equilibrium, the magnitude of shear stress on each pile must decrease inversely with the surface area. This is described by Equation 6.

$$\tau = \frac{\tau_0 r_0}{r} \quad (6)$$

The absolute displacement in pile loading curves has its own practical value, this is because extensometers are usually not installed in the pile nor is there any measurement of soil movement; most measurements are based on absolute displacements of the pile head and, occasionally, also the pile toe.

During the loading process, the pile will displace vertically, and it will shorten. The elastic shortening, obtained by deducting the toe movement from the head movement, will give the minimum relative displacement of pile and soil. The maximum relative displacement possible occurs if the pile head moves but the toe does not move. The real relative movement between pile and soil is somewhere in between these two scenarios. An accurate interpretation can only come from finite element analysis as movement from all elements whether pile or soil can be tracked.

These two extremes represent two possible interpretations of results from actual loading tests; head movement only against head movement minus toe movement at any load. Both interpretations can give different pile behaviours in terms of the pile slip displacements.

The total pile shortening can be taken as a measure of relative displacement, plotted in Figure 27. However, it is then assumed that the entire pile has achieved full mobilization of shaft resistance, and the frictional resistance is neglected.

Figures 28 and 29 show that the normalization of shaft resistance is not possible, due to other mechanics to be further explored.

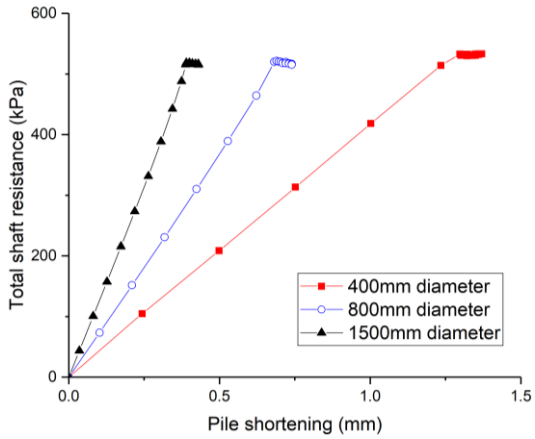

Figure 27 Unit shaft resistance vs. pile shortening

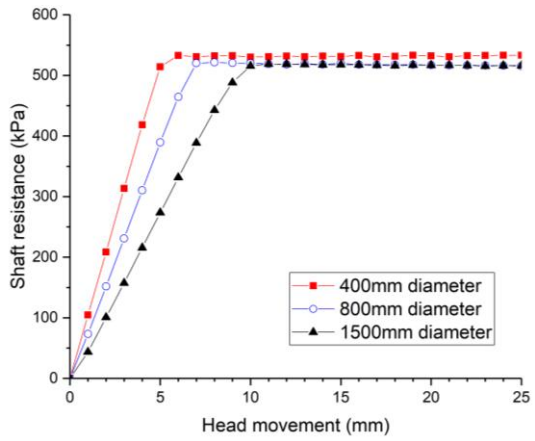

Figure 28 Unit shaft resistance vs. movement

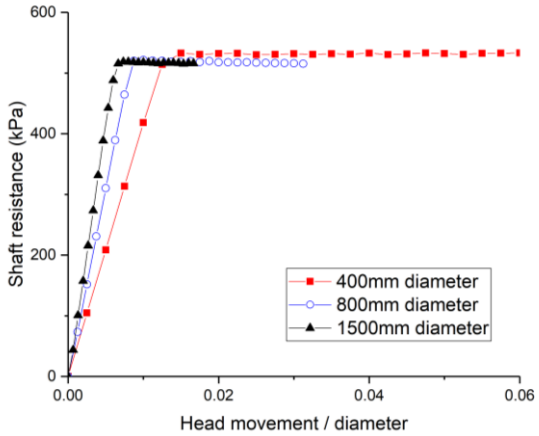

Figure 29 Attempt to normalize unit shaft resistance against head movement divided by the diameter of the pile

4. SINGLE PILE BEHAVIOUR IN HOMOGENOUS SOIL WITH CONSTANT STIFFNESS AND VARYING STRENGTH

The following study follows pile diameters of 400 mm, 800 mm, 1500 mm and 2000 mm, in soil with constant stiffness, and strength that varies with depth (frictional material).

The typical load distribution curve for piles in soil with varying strength with depth does not differ much from the previous section with constant strength, as the same constitutive model is used, Figure 30. However, the rate of mobilisation of the shaft resistance right at the interface boundary between soil and pile varies with depth and pile diameter.

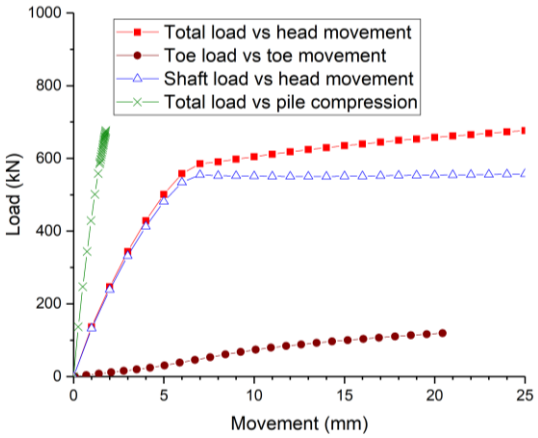

Figure 30 Pile load-movement curve for 400 mm diameter pile in drained soil conditions

Figure 31 plots all the relative movement curves against unit shaft resistance for depths 2.5m, 5m, 7.5m and 12.5m, for the various pile diameters. The interface at the shaft has the same shear stiffness for all the pile depths and diameters. Figure 32 normalizes the shaft resistance against the individual peak resistances.

Grouping the normalized shaft resistance against relative movement curves, the plotted curves by pile size do not give much insight into the pile behaviour. However, when grouped according to pile depth it can be seen that at shallow depth, the slippage occurs at similar values. While at a deeper location, the range where slippage occurs increases slightly. Another observation is that the slip displacement is a function of depth. It is logical that more movement is required to mobilize the peak strength as the deeper soil has a higher maximum strength. When plotting the curves of shaft resistance versus normalized relative movement, Figure 33, it is again shown that the deeper points of the pile require a larger movement to fully mobilize their resistance. However, as the pile diameter increases the range where slip occurs reduces to a much narrower band.

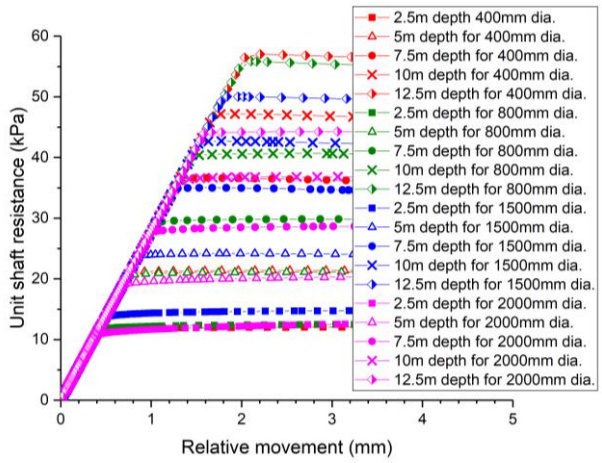

Figure 31 Unit shaft resistance against relative movement curves for various pile diameter at different depths

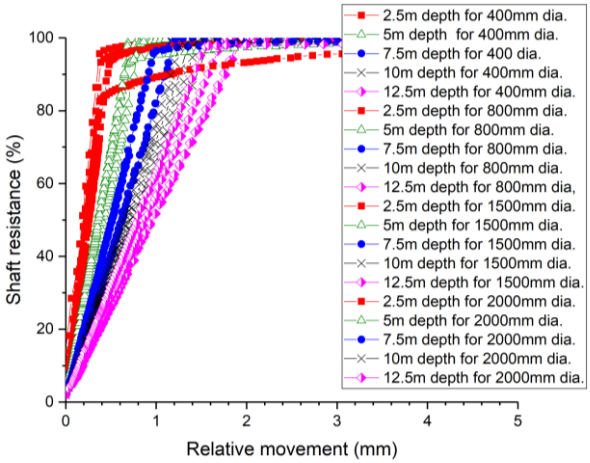

Figure 32 Normalized shaft resistance against relative movement curves for various pile diameter at different depths (grouped according to depth)

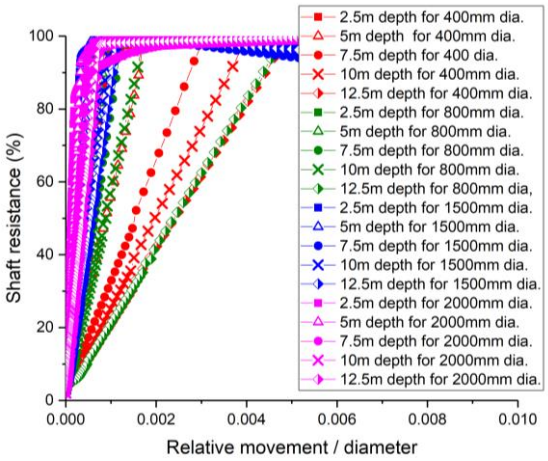

Figure 33 Normalized shaft resistance against normalized relative movement curves for various pile diameter at different depths

Figure 34 shows the toe load-movement curves for the four piles. Converting the plot into a stress vs movement/diameter curve as in Figure 35, it is observed that the smallest pile exhibits the softest

response. During the loading sequence, the piles experience a change in stiffness, piles with smaller diameter more so than those with larger pile diameters. Again, these plots show that when the pile diameter is large, the divergence between the normalized curves decreases.

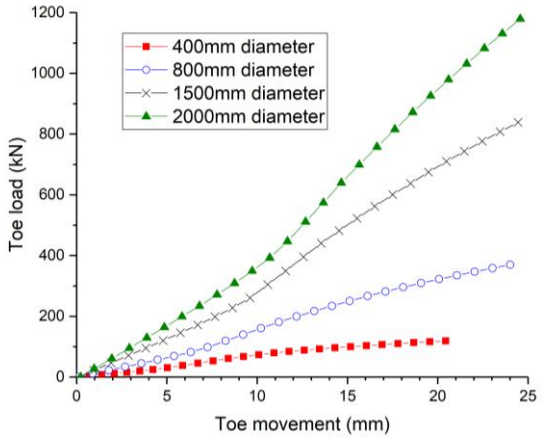

Figure 34 Toe load-movement curves

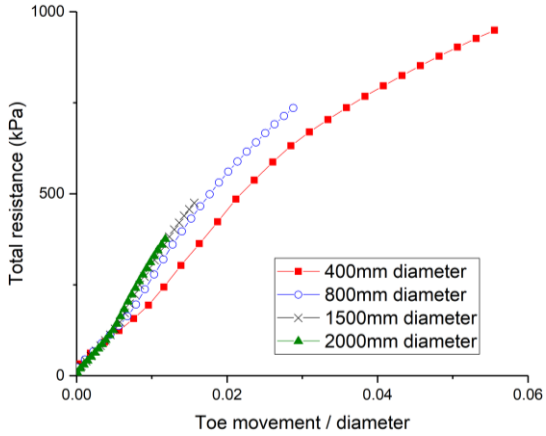

Figure 35 Toe stress vs. normalized toe movement

5. CONCLUDING REMARKS

The paper first discussed about the mechanisms of shallow foundation systems by comparing against homogenous linear elastic, constant strength, and varying strength soil (constant friction angle). The importance of associated and non-associated flow was examined and the contribution from N_c, N_q and N_γ factors were presented. In order to obtain a normalized stress vs movement/diameter curve, associated plasticity and the omission of the N_γ factor were found to be the two key ingredients needed. In that sense, q-z functions may be back-calculated from deep footings on the same soil provided that the stress vs movement/diameter curve can be unique for a given soil.

A single pile was modelled in the same set of homogenous soil and it was shown that t-z and q-z curves can be obtained by tracking the gauss points at the interface and at the toe of the pile. The calculated t-z curve from interface shear stress against movement shows that in a homogenous soil with constant strength, it is possible to use a single t-z function to characterise the pile. In a frictional soil, multiple t-z functions have to be used, depending on the depths along the pile.

The overall shaft resistance against absolute head movement was observed to be a function of diameter and this explains why larger piles would need more movement to mobilise the same stress level, while the rate of mobilisation of shear stress at the interface remains constant in soil with constant strength.

Results from the pile analyses suggest that it is not recommended to adopt a unique q-z curve for the pile toe of different pile diameters on the same soil, especially for frictional materials. The interaction between the pile and soil comprise of complex compressive and shearing responses which make simple normalization difficult, and not absolutely true.

6. REFERENCES

Briaud, J. L., & Gibbens, R. (1997). *Large-scale load tests and data base of spread footings on sand* (No. FHWA-RD-97-068). United States. Federal Highway Administration

Briaud, J. L., & Gibbens, R. (1999). Behavior of five large spread footings in sand. *Journal of Geotechnical and Geoenvironmental Engineering*, *125*(9), 787-796.

Brinkgreve, R. B. J., Kumarswamy, S., Swolfs, W. M. & Foria, F. (2018). PLAXIS 2018 manual. *PLAXIS bv, Delft, Netherlands*.

Fellenius, B. (2019). Basics of foundation design—a textbook. Pile Buck International, Inc., Vero Beach, FL, Electronic Edition, www.Fellenius.net, 484 p.

Fleming, K., Weltman, A., Randolph, M., & Elson, K. (2014). *Piling engineering*. CRC press.

Griffiths, D. V. (1982). Computation of bearing capacity factors using finite elements. *Geotechnique*, *32*(3), 195-202.

Osterberg, J. S. (1947). Discussion in symposium on load tests of bearing capacity of soils. *ASTM STP*, *79*, 128-139.

Palmer, L. (1948, January). Field Loading Tests for the Evaluation of the Wheel-Load Capacities of Airport Pavements. In *Symposium on Load Tests of Bearing Capacity of Soils*. ASTM International.

Skempton, A. W. (1951). The bearing capacity of clays. In *Proc. of Building Research Congress* (Vol. 1, pp. 180-189). ICE.

Terzaghi, K. (1943), Theoretical soil mechanics, Wiley, New York.